Available online at www.sciencedirect.com
ScienceDirect
Engineering Failure Analysis 15 (2008) 989–999
ENGINEERING FAILURE ANALYSIS
www.elsevier.com/locate/engfailanal

Review

Safety evaluation of table liner for vertical roller mill by modified fatigue limit

Dong-Woo Lee [a], Seok-Swoo Cho [b], Won-Sik Joo [a,*]

[a] Department of Mechanical Engineering, Dong-A University, Busan, Republic of Korea
[b] Department of Vehicle Engineering, Kangwon National University, Samcheok, Republic of Korea

Received 23 March 2007; accepted 24 April 2007
Available online 13 May 2007

Abstract

The vertical roller mill is a device in the grinding process of portland cement. On the result of component preventive maintenance, the table liner for the vertical roller mill was fractured before the designed life of vertical roller mill which is (4×10^7) cycles. In this study we found out the fracture mechanism of the table liner using HDM and FEA, and estimated its safety using Goodman diagram.

Keywords: Goodman diagram; HDM; SIF; Table liner; Vertical roller mill

Contents

* Corresponding author. Tel.: +82 51 200 7641; fax: +82 51 200 7656.
E-mail address: woooow@donga.ac.kr (W.-S. Joo).

1350-6307/$ - see front matter © 2007 Elsevier Ltd. All rights reserved.
doi:10.1016/j.engfailanal.2007.04.008

1. Introduction

The vertical roller mill is an expensive device to produce portland cement. But on the result of component preventive maintenance, the table liner for the vertical roller mill was fractured before the designed life of the vertical roller mill which is (4×10^7) cycles. The repair expense of the table liner accounts for 30% of all the repair expense of the vertical roller mill [1].

Failure analysis of fractured engineering structures generally uses fracture mechanics. Several studies about the fracture mechanism of structures by SEM or X-ray methods have been reported. Nishijima et al. [2] studied that the repeated stress on the airplane propeller composed of blade and hub could be estimated using optical microscope and SEM. But, this method can not be applied to the contaminated fracture surface. Chiaki et al. [3] showed the fact that the past operation load applied to the fractured automobile connecting rod could be determined by the X-ray residual stress. X-ray fractography has limited applications because of material crystal size, difficult measurement method, electrolytic polishing precision, and long test time.

Therefore, this study found out the fracture mechanism of the table liner using HDM and estimated its safety using Goodman diagram.

2. Failure accident of table liner for vertical roller mill

Fig. 1 shows schematic diagram of a vertical roller mill used for portland cement production. It is composed of several rollers, rotational table liner, grounding bowl, and hydraulic cylinders. Fig. 2 shows the table

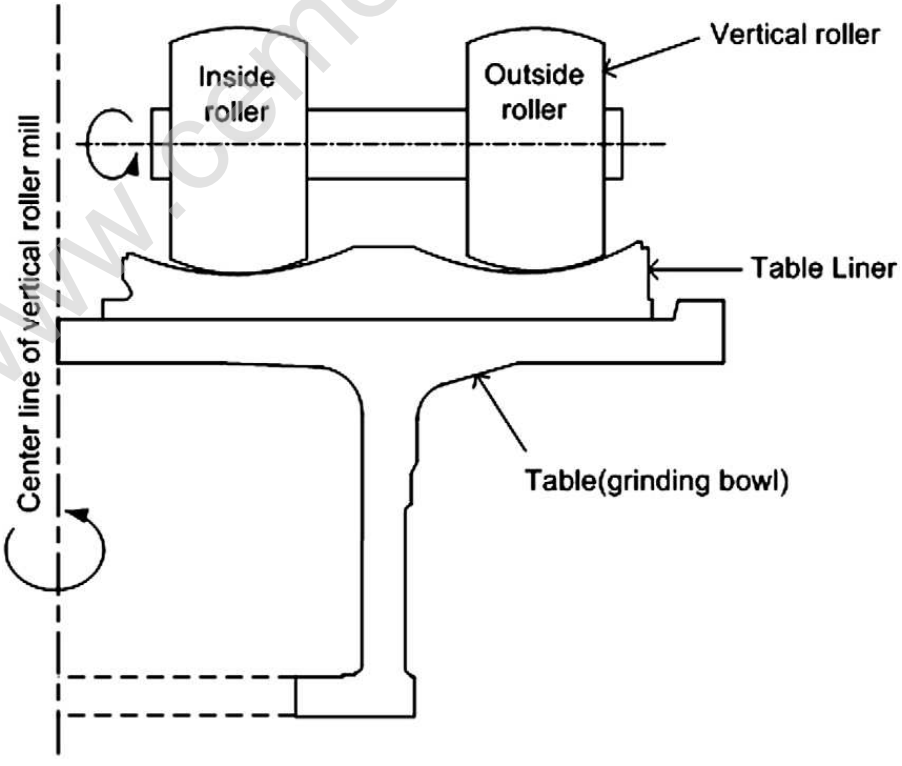

Fig. 1. Schematic diagram of vertical roller mill for Portland cement.

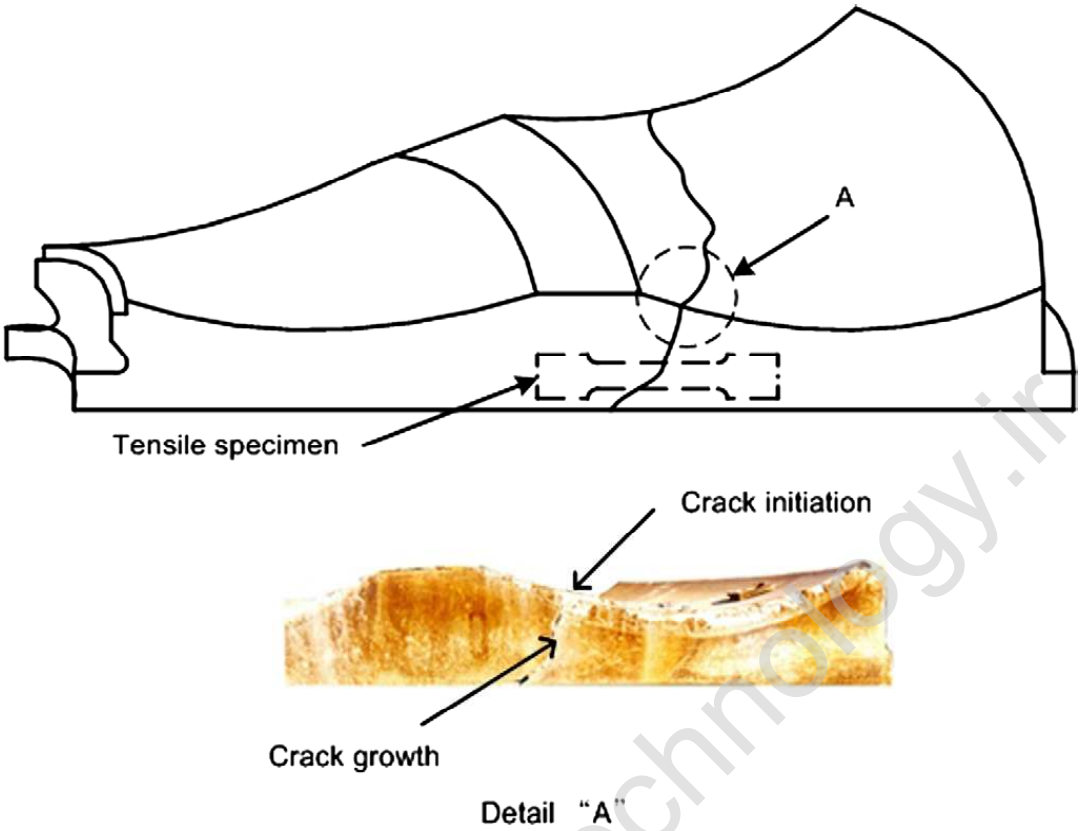

Fig. 2. Sampling direction of tensile and bending specimen and fracture process of table liner.

liner geometry and its failure location. Examination of a failed table liner indicated that the fatigue crack initiated at the outer corner and propagated simultaneously in circumferential and axial directions.

3. Experimental procedures

3.1. Material properties

Fig. 2 shows the tensile specimen that was cut from fractured components. It was cut in a radial direction by taking into consideration the fracture pattern of the table liner. The electro–mechanical system with 98 kN capacity (INSTRON model 1337) was conducted to perform the tensile test. The tensile strain was measured using the extensometer with a 25 mm gage length (INSTRON model 1337 2630-004). A chemical analysis of the material (SC450 steel) that was obtained from the undamaged part of the table liner is given in Table 1. Table 2 shows the mechanical properties of SC450 steel. The used material has good yield strength, tensile strength and elongation which fall under the recommended value.

3.2. Fatigue crack growth test

Fatigue crack growth tests were carried out according to ASTM E 647-95 standard using the electro–mechanical test system with 98 kN capacity (INSTRON model 1337) [4]. All fatigue crack growth tests were

Table 1
Chemical composition of SC450 steel (wt.%)

C	Cr	Si	Mn	Ni	P	S
0.22	0.10	0.8	0.7	0.015	0.04	0.06

Table 2
Mechanical properties of SC450 steel

Properties	Unused	Used
Yield strength σ_{ys} (MPa)	238.2	241.6
Tensile strength σ_{ts} (MPa)	480	474
Poisson's ratio v	0.300	0.306
Elongation ε_f (%)	24	22.7
Young's modulus E (GPa)	203	206
Density ρ (kg/mm^3)	7.85×10^{-6}	7.85×10^{-6}

performed at 0.13 and 0.3 R-ratios under sinusoidal loading waveform. The repeated load was controlled as a constant loading amplitude at an operating frequency (10 Hz). Fig. 3 shows the geometry of SEB (Single EdgeCracked Pure Bend) specimen [5]. Crack length was measured on both the specimen surfaces using a low power traveling microscope (×50). Crack growth rate was obtained with the scent method. The stress intensity factor K for a single edge crack of this configuration is given by Eq. (1) [5].

$$K_I = (6M/BW^2)(\pi a)^{1/2}(1.122)1.40(a/W) + 7.77(a/W)^2 - 12.08(a/W)^3 + 14.0(a/W)^4 \quad (1)$$

where, M is moment, W is specimen width, B is specimen thickness, and a is crack length.

3.3. Distribution of residual stress beneath the fracture surface

3.3.1. Test apparatus and procedure

The residual stress on the fracture surface was determined by RS-200 (Micro-Measurements Group). To avoid the errors between the center of the drilled hole and the center of the strain gage circle, milling guide and high speed air turbine system were used for centering the tool holder. The rosette strain gage (Micro measurement) was placed in the area under consideration. Residual strain is relieved when a hole is drilled at the geometrical center of it. The residual stress is related to the relieved strain. The diameter and the depth of the drilled hole were determined by ASTM E 837-99 [6].

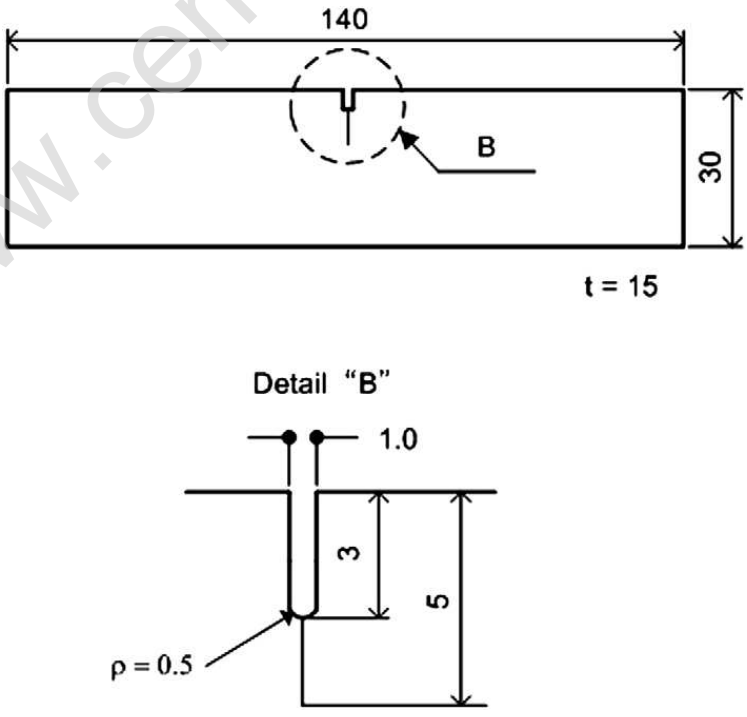

Fig. 3. Geometry and dimension of SEB specimen of SC450 steel (unit: mm).

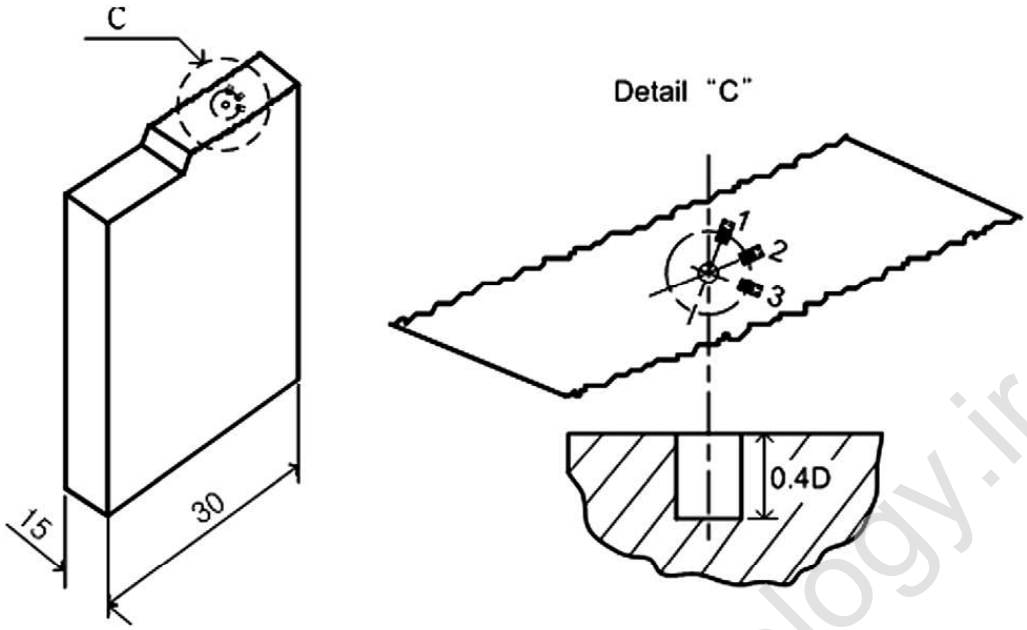

Fig. 4. Schematic illustration of HDM on fatigue fractured surface of SEB.

Fig. 5. View of HDM attached to fatigue fractured surface of table liner.

3.3.2. Test specimen

3.3.2.1. Fatigue crack growth test. Fig. 4 shows the attachment position of the strain gage on the fatigue fracture surface. The measurements of plastic zone depth were performed in the direction of crack growth and at different locations which corresponded to various K_{max} values ($R = 0.13 - K_{max} = 14.28,\ 26.66\ \mathrm{MPa}\sqrt{m}$, $R = 0.3 - K_{max} = 14.28,\ 20.47\ \mathrm{MPa}\sqrt{m}$). In this study, we defined the plastic zone depth as the vertical distance from the fracture surface to the position which makes the relieved strain a constant.

3.3.2.2. Fractured table liner. Fig. 5 shows the hole drilling apparatus on the fracture surface of the table liner. In this study, we defined the plastic zone depth as the vertical distance from the fracture surface to the position which makes the relieved strain a constant.

4. Experimental results and discussion

4.1. Distribution of the relieved strain on the fatigue fracture surface

Fig. 6 shows the variation of the relieved strain against the hole depth of the fracture surface. The relieved strains were founds to decrease up to a hole depth below the fracture surface, followed by a constant value

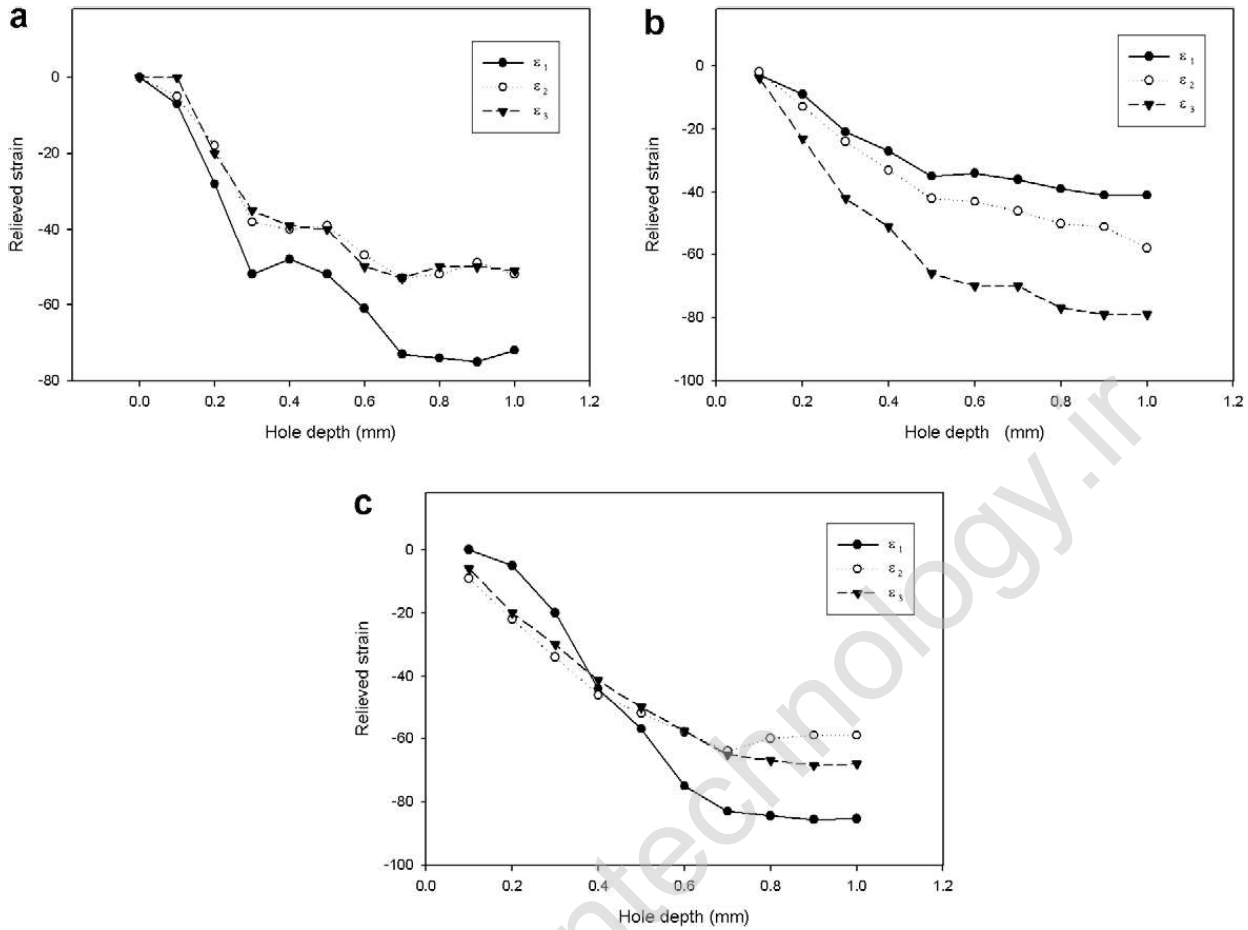

Fig. 6. Relieved strain plotted against the depth from fatigue fractured surface for SEB (a) $K_{max} = 14.28$ MPa $m^{1/2}$, (b) $K_{max} = 20.47$ MPa $m^{1/2}$ and (c) $K_{max} = 26.66$ MPa $m^{1/2}$.

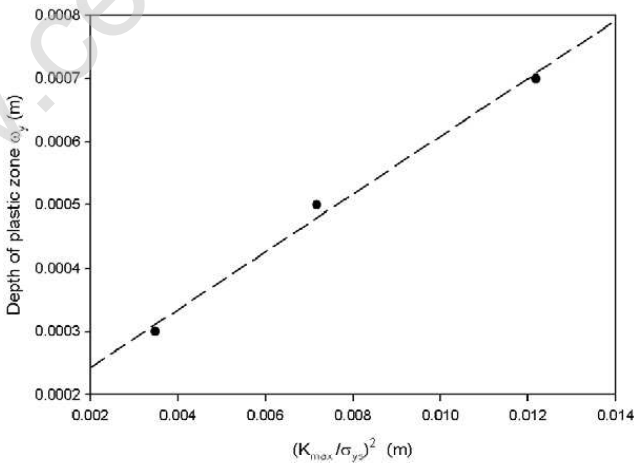

Fig. 7. Relationship between plastic zone depth and maximum stress intensity factor to yield strength.

thereafter. The hole depth from the fracture surface at which the relieved strain reaches a constant value is designated as the plastic zone depth. The plastic zone depths for $K_{max} = 14.28$, 20.47, 26.66 MPa$\sqrt{m}$ were found to be 0.3, 0.5, 0.7 mm, respectively.

4.2. Relationship between plastic zone depth and maximum stress intensity factor

The most promising application of this method is found in the determination of the monotonic plastic zone size ω_y. It was found that the values ω_y determined through the sub-surface analysis at different locations on the fracture surface are in good agreement with the predicted values ω_y according to the relationship below [7,8].

$$\omega_y = \alpha(K_{max}/\sigma_{ys})^2 \tag{2}$$

where, σ_{ys} is yielding stress, α is material constant, and K_{max} is maximum stress intensity factor.

In most of these investigations, a linear relationship was reported between the values from the sub-surface analysis and $(K_{max}/\sigma_{ys})^2$. For the case of this experiment, the α value obtained by least square method is 0.0457 (see Fig. 7).

5. Quantitative fatigue analysis of the failed table liner

The residual stress observation of fracture surface yields useful information to analyse the causes of failure accidents of engineering structures. Fatigue crack initiation, propagation, and final fracture marks as broad distinctive features are identified clearly just by visual observation. The initiation of the fatigue crack in the table liner is considered to be the result of local stress concentration between it and the roller. It may assume that the measurement position of the plastic zone depth on the fracture surface can become fatigue crack initiation site in view of the loading type applied to it. Fig. 8 shows the relationship between the hole depth and the relieved strains in the table liner. The relieved strains at the fracture surface was decreased with the direction of the depth and approached constant values approximately at $\omega_y = 500\ \mu m$. We can predict $K_{max} = 25.3\ MPa\sqrt{m}$ by substituting $\omega_y = 500\ \mu m$ into Eq. (2). Fig. 9 shows the geometry of stress intensity factor under bending load. The form of the stress intensity factor K is given by Eq. (3) [9].

$$\begin{aligned}
&K_A = \sigma_b\sqrt{\pi b}\cdot(M/\Phi)\cdot H_2, \quad K_B = \sigma_b\sqrt{\pi b}\cdot(M/\Phi)\cdot SH_1\\
&M = (1.13-0.09\lambda)+\left(-0.54+\frac{0.89}{0.2+\lambda}\right)\beta^2+\left\{0.5-\frac{1}{0.65+\lambda}+14.0(1-\lambda)^{24}\right\}\beta^4\\
&\Phi^2 = 1+1.464\lambda^{1.65}\\
&S = (1.1+0.35\beta^2)\sqrt{\lambda}\\
&H_2 = 1-(1.22+0.12\lambda)\beta+(0.55-1.05\lambda^{0.75}+0.47\lambda^{1.5})\beta^2\\
&H_1 = 1-(0.34+0.11\lambda)\beta\\
&b/a = \lambda\\
&b/t = \beta
\end{aligned} \tag{3}$$

where, a and b are crack length and t is specimen thickness.

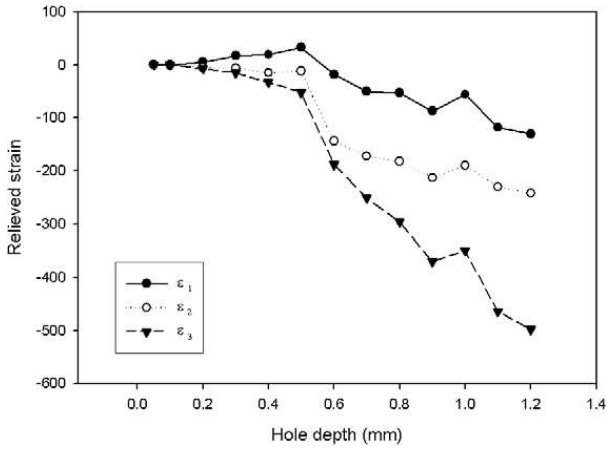

Fig. 8. Relieved strain plotted against the depth from fatigue fractured surface for table liner.

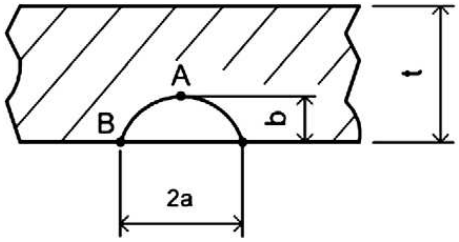

Fig. 9. Geometry of stress intensity factor under bending loads.

From the crack shape of the initiation site, the coefficients were measured as follows.

$$a = 0.0256\ \text{m}, \quad b = 0.02\ \text{m}, \quad t = 0.423\ \text{m} \tag{4}$$

In Eq. (4), the plate thickness t was regarded as a table liner thickness. We could obtain the maximum stress 142.4 MPa at the crack surface site using $K_{\max} = 25.3\ \text{MPa}\sqrt{m}$ and Eq. (3).

6. Failure load of the table liner

The regression equation between the applied load and the stress can be obtained by the FEA results on the table liner. On the basis of the above results, the maximum load applied to the table liner can be determined using the regression equation. Fig. 10 and Eq. (5) show the regression results. The load applied to the table liner is expected to be 11.3 MN and 4 times more than design load 2.9 MN.

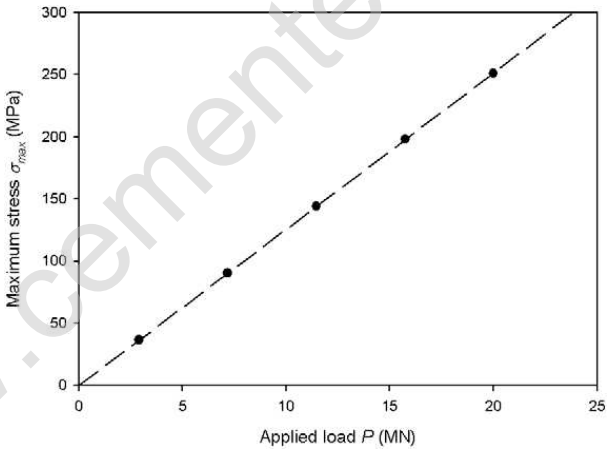

Fig. 10. Relation between load and maximum stress for table liner.

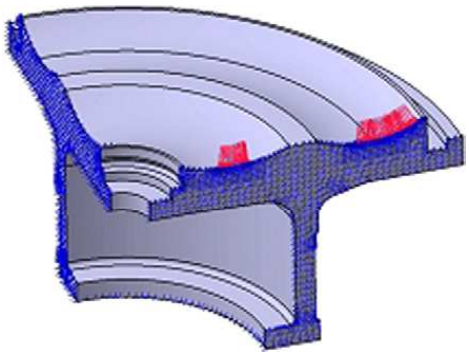

Fig. 11. Load and boundary conditions of vertical roller mill.

Table 3
Analysis results of vertical roller mill

	Load position		Von Mises stress	
	Inside (MN)	Outside (MN)	σ_{min} (MPa)	σ_{max} (MPa)
Design load	1.1	2.9	0.00594	36.78
Failure load	1.1	11.3	0.05834	142.40

$$P = (\sigma_{max} - 0.5282)/12.518 \quad (5)$$

where, P is applied load and σ_{max} is maximum stress.

Finite element analysis was carried out by linear analysis solver of CATIA V5.9. Fig. 11 shows loading condition and boundary condition used in FEA. We use the quarter FE model considering the geometry and the loading of the vertical roller mill. The failure load is applied to the contact area between the mill and the roller. Table 3 summarizes the results of FEA for vertical roller mill.

7. Safety evaluation of the table liner

7.1. Safety evaluation by no modified fatigue limit

Fig. 12 shows Goodman endurance diagram [10] for the table liner. A safe domain was bounded by a limit line in the form of a straight line through four limit points taken from the test results $-\Delta\sigma = 182$ MPa, $\sigma_{ys} = 241.6$ MPa, and $\sigma_{ut} = 474$ MPa. Design stress could be obtained by FEA under design and failure stress could be obtained by FEA under failure load. The circle symbol and square symbol indicate design stress ($\Delta\sigma = 18.39$ MPa, $\sigma_{mean} = 18.39$ MPa) and failure stress ($\Delta\sigma = 71.24$ MPa, $\sigma_{mean} = 71.17$ MPa), respectively. The table liner is safe because stresses remain within the limit diagram. This result can be attributed to the definite difference between the fatigue limit in a material and that in a component. It is necessary to modify the fatigue limit in order to estimate the safety of the table liner precisely.

7.2. Safety evaluation by modified fatigue limit

The fatigue limit of a machine part depends strongly on its various conditions (surface roughness, material structure, residual stress, and processing method). The correlation of the fatigue limit and some of the factors can be expressed by the empirical equation. To account for the importance of these conditions, we employ a variety of modifying factors, each of which is intended to account for a single effect. Using this idea, we may write

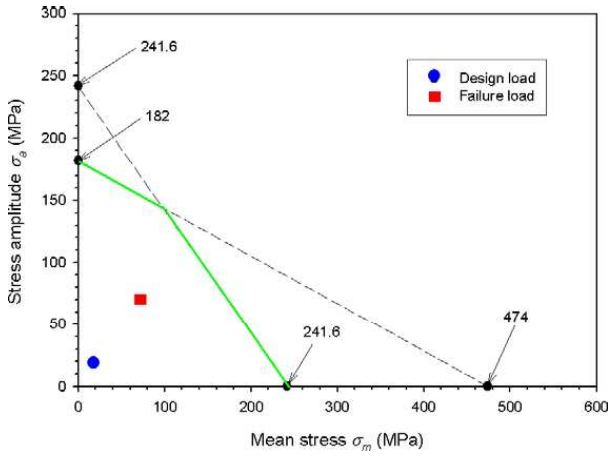

Fig. 12. Goodman diagram for table liner by standard fatigue limit.

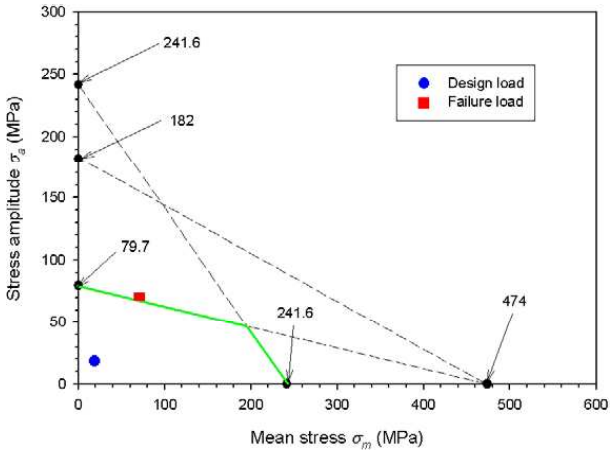

Fig. 13. Goodman diagram for table liner by modified fatigue limit.

$$S_e = C_{load} C_{size} C_{surf} C_{temp} C_{reliab} S'_e \tag{6}$$

where S_e is fatigue limit of the table liner and S'_e is fatigue limit of SC450 steel ($R = -1$).

The load factor C_{load} has been evaluated according to loading types. For bending, we obtain $C_{load} = 1$. The size factor C_{size} has been evaluated according to loading types and structure scale. Shigley and Mitchell [11] proposed that for large-scale component, C_{size} had 0.6 for bending and torsion. Therefore, we obtain $C_{size} = 0.6$.

The surface of the test specimen is highly polished, with a final polishing in the axial direction to smooth out any circumferential scratches. The modification factors depend upon the quality of the finish. In Juvinall graph [12], the surface factor C_{surf} indicates 0.814 for coarse finished surface treatment. Therefore, we obtain $C_{surf} = 0.814$.

The temperature of the operation may have a significant influence on the fatigue strength. Generally speaking, the fatigue strength is enhanced at temperatures below room temperature and diminished at temperatures above room temperature, although exceptions may be found. Shigley and Mitchell [13] proposed that the temperature factor C_{temp} was 1 for the operating temperature below 450. We obtain $C_{temp} = 1$ because the table liner is operated at 260 °C.

It is reasonable to expect that there will be scatters in the material strengths of each of the individual test specimens. Haugen and Wirsching et al. [14] proposed that the standard deviation of fatigue limit in steel did not exceed 8% of average fatigue limit. From the above results, we obtain $C_{reliab} = 0.897$ for 90% confidence limit.

If we substitute the above factors into Eq. (6), we obtain modified fatigue limit 79.7 MPa. When all the modifying factors are considered, fatigue limit dropped by 56.2%.

Fig. 13 shows Goodman endurance diagram using modified fatigue limit. Design stresses come into the limit diagram but failure stresses exist out of it. Therefore, for an infinite fatigue life, the table liner must be designed to assure the working stresses due to loading are within the endurance diagram by modified fatigue limit.

8. Conclusion

This study performed failure analysis using HDM and fatigue analysis in order to estimate the safety of the table liner for vertical roller mill. Main results were obtained as follows.

1. From fatigue crack growth test of SC450 steel, the relation between plastic zone depth and the maximum stress intensity factor divided by the monotonic yielding strength K_{max}/σ_{ys} is given by

$$\omega_y = 0.0457\ (K_{max}/\sigma_{ys})^2$$

2. We could obtain the maximum stress 142.4 MPa and the maximum stress intensity factor $K_{max} = 25.3\ \mathrm{MPa}\sqrt{m}$ at the crack surface site using HDM and fatigue analysis.
3. For an infinite fatigue life, the table liner must be designed to assure the working stresses due to loading are within the endurance diagram by modified fatigue limit.

References

[1] Tongyang Cement Co. Maintenance of table liner for vertical roller mill. 1993;16–9.
[2] Minoshima K, Endo M, Miyawaki T, Komai K. Three dimensional quantitative analysis of brittle fracture surface with SEM/STM/AFM. JSME 1995;67(2):1587–94.
[3] Chiaki Tsubouchi, Takeshi Horikawa. Analysis of Connecting rod fatigue fracture surface by X-ray fractography. J Soc Mater Sci, Jpn 2000;49(10):1143–7.
[4] ASTM E647-95. Standard test method for measurement of fatigue crack growth rates. ASTM standards Sec.3 1995;3(1):591–6.
[5] Gross B, Srawley JE. Stress intensity factor for single-edge-notch specimens in bending or combined bending and tension by boundary collocation of a stress function. NASA, Technical Note 1965; D-2603.
[6] ASTM E837-99. Standard test method for determining residual stresses by the hole-drilling strain-gage method. Annual Book of ASTM 1999:1–6.
[7] Levy N, Marcal PV, Ostengren WJ, Rice JR. Int J Fract Mech 1971;7:143.
[8] Boo MH, Park YC, Yun DP, Huh SC, Kim TH. Evaluation of fracture mechanics parameter using X-ray fractography method of WC-Co cemented carbides. J KSME 1999;23(10):1709–15.
[9] Newman Jr. JC, Raju IS. Analysis of surface cracks in finite plates under tension or bending loads. NASA, Technical note 1979;TP-1578.
[10] Smith JO. The effect of range of stress on the fatigue strength of metals. Univ of Ill, Eng Exp Sta Bull 1942:334.
[11] Shigley JE, Mitchell LD. Mechanical engineering design. 4th ed. New York: McGraw-Hill; 1983. 293.
[12] Jubvinall RC. Engineering considerations of stress, strain and strength. New York: McGraw-Hill; 1967. 233–4.
[13] Shigley JE, Mitchell LD. Mechanical engineering design. 4th ed. New York: McGraw-Hill; 1983. 300.
[14] Haugen EB, Wirsching PH. Probabilistic design, Machine design 47:10–4.